IEEE Access
Multidisciplinary : Rapid Review : Open Access Journal

Received March 14, 2020, accepted March 26, 2020, date of publication March 31, 2020, date of current version April 15, 2020.

Digital Object Identifier 10.1109/ACCESS.2020.2984590

Research of NSMDOB-Based Compound Control for Photoelectric Tracking Platform

YAN REN[1,2], DAPENG TIAN[2], (Senior Member, IEEE), AND DAHUA YU[1]
[1]Information Engineering School, Inner Mongolia University of Science and Technology, Baotou 014010, China
[2]Key Laboratory of Airborne Optical Imaging and Measurement, Changchun Institute of Optics, Fine Mechanics and Physics, Chinese Academy of Sciences, Changchun 130033, China

Corresponding authors: Dapeng Tian (d.tian@ciomp.ac.cn) and Dahua Yu (fmydh@imust.edu.cn)

This work was supported in part by the National Natural Science Foundation of China under Grant 61563041, Grant 61673365, Grant 81571753, and Grant 81871430, in part by the Inner Mongolia Natural Science Foundation under Grant 2019MS06002, in part by the Ministry of Education Chunhui Plan Science Research Foundation, and in part by the Key Laboratory of Airborne Optical Imaging and Measurement of Chinese Academy of Sciences Open Foundation.

ABSTRACT Disturbance compensation is an important criteria to evaluate the performance of a photoelectric tracking servo control system. In order to effectively compensated disturbance in high frequency, a novel sliding mode disturbance observer (NSMDOB) is proposed in this paper. The dynamic performance of the system is improved by the design of the compound control scheme with the NSMDOB and additive decomposition theory. According to the additive decomposition theory, the photoelectric tracking platform servo system was decomposed into the main system and the auxiliary system. The tracking control and disturbance compensation were considered respectively in two systems. A rapid switching technique of the sliding mode was used to estimate the high frequency disturbance in the NSMDOB and the compensator of the auxiliary system. Finite-time control (FTC) was used to design the sliding mode compensator, which could maintain the state of auxiliary system asymptotically stable. Experiment results prove that the proposed method may offer the fast convergence rate, the high tracking accuracy, and the strong robustness of the control system.

INDEX TERMS Novel sliding mode disturbance observer, finite-time control, photoelectric tracking platform, additive decomposition, sliding mode control.

I. INTRODUCTION

Photoelectric tracking system is a kind of typical servo system. Photoelectric tracking stabilization platform may isolate the carrier disturbance, measure the change of platform posture and position continuously, maintain the dynamic attitude reference accurately, and realize to track the moving target through the image detection equipment [1]. In the photoelectric imaging system, the Line of Sight (LOS) stabilization of photoelectric tracking platforms determines the image quality of the photoelectric device directly [2], [3].

It is key problem how to ensure the LOS stabilization of photoelectric tracking platforms. The disturbances, including the uncertainty of mechanism, nonlinear friction between frameworks, the vibration of carrier attitude and the wind resistance torque in flight, may cause the LOS instability of the photoelectric tracking platform. Photoelectric tracking stabilization platform is a typical nonlinear and strong coupling servo control system, which contains multi-source disturbance. The LOS stabilization and the moving target tracking may be converted into two control problem in photoelectric tracking system, which are the disturbance compensation and the tracking control.

Disturbance Observer (DOB) can be divided into the linear disturbance observer and the nonlinear disturbance observer. As a disturbance compensation method, DOB is widely used in the motion control field for its simple and facile realization [4]–[7]. She et al. proposed the concept of Equivalent Input Disturbance (EID) and designed a disturbance compensation method to suppress disturbances [8]. The estimation value of system state is used to solve the estimation value of EID, which may achieve the compensation of EID [9], [10]. The traditional disturbance observer can effectively estimate and compensate the slow-varying disturbance. Previous studies utilized the fast switching characteristic of sliding mode control to design the Sliding Mode Disturbance

The associate editor coordinating the review of this manuscript and approving it for publication was Ailong Wu.

Observer (SDOB), which solves the application limitation of the traditional disturbance observer [11]–[13]. The method needs to get specific structural forms of disturbance, which may be applied to the compensation for a certain kind of disturbance [9]. Moreover, some scholars also proposed the design methods of fuzzy disturbance observer and neural network disturbance observer, which are difficult to realize in engineering practice [14], [15].

The control system of photoelectric tracking platform should have the following characteristics, including fast response, small tracking error and strong anti-interference ability etc. It is important to improve the dynamic performance of servo system that the tracking accuracy and robustness of the system can be quantitatively analyzed. Finite-Time Control (FTC) is an effective method to solve the kind of fast and stable control problem [16]–[18]. Sliding mode control has the characteristic of fast switching variable structure. It is effectively to improve the system performance that the sliding mode control combines with the advanced control methods such as adaptive control, intelligent control and FTC [19]–[22]. According to additive decomposition theory, the states of system can be decomposed into the sum of two subsystems states. One subsystem can be arbitrary designed and the other one can be described as the difference between the system and the designed subsystem [23], [24]. The additive decomposition theory has been successfully applied in many fields since it may Separate control target [25]–[28].

In present study, we present a compound control approach to compensate for the disturbance and improve the performance in the photoelectric tracking stabilization platform based on the additive decomposition theory. A novel sliding mode disturbance observer (NSMDOB) was designed to estimate the disturbance based on the EID concept, which utilizes linear information in system to estimate nonlinear disturbance. In order to realize the fine disturbance compensation for the disturbance and separate control tasks, we used the additive decomposition theory to decompose the system with the NSMDOB into the main system and auxiliary system. The disturbance compensation and the tracking control were considered separately in the system. The advantages of sliding mode control were combined with the FTC theory to design the compensator in the auxiliary system. The NSMDOB and compensator realized the fine disturbance compensation and improve the robustness of the system. The tracking controller was designed to guarantee the position responses accuracy in the main system. Therefore, the LOS stabilization and moving target tracking may be designed independently. This paper demonstrates the value of the compound control approach, which can achieve the effective compensation for the disturbance and improve the tracking accuracy.

The paper is organized as follows. Sec. II proposes the sliding mode disturbance observer based on the EID concept. Sec. III adopts the additive decomposition theory to decompose the system structure after system disturbance compensation. Sec. IV presents a detail design and analysis about the design of controller of main system and compensator of auxiliary system. Sec. V describes the experiment. Finally, Sec. VI concludes the paper.

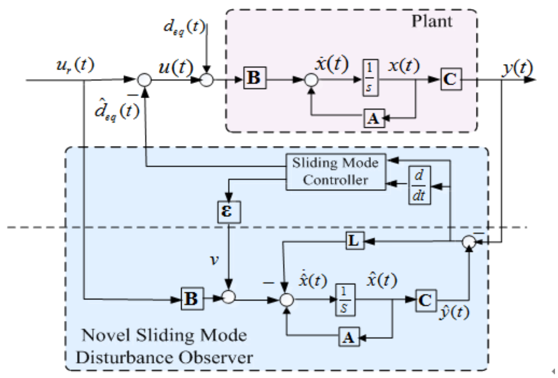

FIGURE 1. NSMDOB control structure.

II. SLIDING MODE DISTURBANCE OBSERVER

The disturbance may be imposed on a channel other than the control input channel, and the number of the disturbance associated with input channels may also be larger than one. According to the definition of EID in the references [8], a plant with the actual disturbance $d(t)$ can be interpreted as a plant with an EID $d_{eq}(t)$. The single-input and single-output linear system can be described as

$$\begin{cases} \dot{\mathbf{x}}(t) = \mathbf{A}\mathbf{x}(t) + \mathbf{B}[u + d_{eq}(t)] \\ y(t) = \mathbf{C}\mathbf{x}(t) \end{cases} \tag{1}$$

where, $\mathbf{x} \in \Re^n$, $\mathbf{A} \in \Re^{n\times n}$, $\mathbf{B} \in \Re^n$, $\mathbf{C} \in \Re^{n_y \times n}$, $\mathbf{u} \in \Re$, and $\mathbf{y} \in \Re$.

A. DESIGN OF SLIDING MODE DISTURBANCE OBSERVER

DOB should consider the realization of the system inverse model. The paper proposes NSMDOB to estimate the EID, which of structure is shown in Fig. 1. The NSMDOB uses the state observer of linear system to replace the inverse model of the system nominal model in DOB. It is avoided that the inverse model is not existence.

The following assumptions are made about the plant.

Assumption 1: ($\mathbf{A}$, $\mathbf{B}$, $\mathbf{C}$) are controllable and observable.

According to the assumption, there are positive definite symmetric matrices $\mathbf{P}$, $\mathbf{Q}$ and matrice $\mathbf{K}$ with appropriate dimension, which satisfy the following equation $(\mathbf{A} - \mathbf{BK})^{\mathrm{T}}\mathbf{P} + \mathbf{P}(\mathbf{A} - \mathbf{BK}) = -\mathbf{Q}$.

Assumption 2: EID d_{eq} is norm bounded. There is a positive number d_M that $\left\| d_{eq} \right\| \le d_M$ is met.

The NSMDOB of the plant (1) is designed as

$$\begin{cases} \dot{\hat{\mathbf{X}}} = \mathbf{A}\hat{\mathbf{X}} + \mathbf{B}u_r - \mathbf{LC}(\hat{\mathbf{X}} - \mathbf{X}) - \mathbf{v} \\ \mathbf{v} = \boldsymbol{\varepsilon}\mathrm{sgn}(S) \end{cases} \tag{2}$$

where S is the sliding mode surface function which is described as (6), $\boldsymbol{\varepsilon} \in \Re^n$ is the switching gain constant matrix, and $\mathbf{L} \in \Re^{n \times n_y}$ is observer gain matrix. The observer reproduces the state of the plant $\hat{\mathbf{X}}$, its output is $\hat{\mathbf{y}}$ and u_r is the controller output.

If we let $r(t) = 0$ and $d_{eq}(t) = 0$, then the plant (1) is

$$\dot{\mathbf{X}} = \mathbf{AX} + \mathbf{B}u \tag{3}$$

The control law is design as (4)

$$u = u_r - \hat{d}_{eq} \tag{4}$$

where $\hat{d}_{eq}$ is the output of NSMDOB, namely the estimation of the EID.

Let $\mathbf{E} = \hat{\mathbf{x}} - \mathbf{x}$. Combing (2), (3) and (4) with aforementioned equation yields

$$\dot{\mathbf{E}} = (\mathbf{A} - \mathbf{LC})\mathbf{E} + \mathbf{B}\hat{d}_{eq}(t) - \mathbf{v} \tag{5}$$

According to the feedback control theory, an integral sliding mode surface function with the error of the observer is adopted

$$S = \mathbf{H}(\mathbf{E} - \int_0^t (\mathbf{A} - \mathbf{BK})\mathbf{E}(\tau)d\tau) \tag{6}$$

where $\mathbf{K} \in \Re^{n_u \times n}$ is the sliding mode surface feedback gain matrix, and $\mathbf{H} \in \Re^{n}$ is the positive constant matrix.

$$\begin{aligned}\dot{S} &= \mathbf{H}[\dot{\mathbf{E}} - (\mathbf{A} - \mathbf{BK})\mathbf{E}] \\ &= \mathbf{H}[(\mathbf{A} - \mathbf{LC})\mathbf{E} + \mathbf{B}\hat{d}_{eq}(t) - \mathbf{v} - (\mathbf{A} - \mathbf{BK})\mathbf{E}] \\ &= -\mathbf{H}(\mathbf{LC} - \mathbf{BK})\mathbf{E} + \mathbf{HB}\hat{d}_{eq}(t) - \mathbf{Hv}\end{aligned} \tag{7}$$

When the system enters the sliding mode motion, $\dot{S} = 0$ is met. If $\mathbf{HB}$ meets reversible, then $\hat{d}_{eq}$ is described as

$$\hat{d}_{eq} = (\mathbf{HB})^{-1}\mathbf{H}(\mathbf{LC} - \mathbf{BK})\mathbf{E} + (\mathbf{HB})^{-1}\mathbf{Hv} \tag{8}$$

Theorem 1: For system (1) with uncertain disturbance, design parameter matrix $\mathbf{L}$ and $\mathbf{K}$, and makes $\mathbf{A} - \mathbf{LC}$ and $\mathbf{A} - \mathbf{BK}$ to be the Hurwitz matrix. If NSMDOB is designed as (2), the sliding mode surface is (6) and the control law is (10), then the NSMDOB is asymptotically stable. The NSMDOB can effectively estimate the EID $d_{eq}(t)$ in the system (1).

Proof: Define a Lyapunov candidate $V_o = \mathbf{E}^{\mathrm{T}}\mathbf{PE} + \frac{1}{2}S^2$, where $\mathbf{P}$ is a positive definite symmetric matrix. Then, according to (2), (6) and (10) , the time derivative of V_o is deduced as (11).

$$\begin{aligned}\dot{V}_o &= \dot{\mathbf{E}}^{\mathrm{T}}\mathbf{PE} + \mathbf{E}^{\mathrm{T}}\mathbf{P}\dot{\mathbf{E}} + S\dot{S} \\ &= [(\mathbf{A} - \mathbf{LC})\mathbf{E} + \mathbf{B}\hat{d}_{eq} - \mathbf{v}]^{\mathrm{T}}\mathbf{PE} + \mathbf{E}^{\mathrm{T}}\mathbf{P}[(\mathbf{A} - \mathbf{LC})\mathbf{E} \\ &\quad + \mathbf{B}\hat{d}_{eq} - \mathbf{v}] + S(\mathbf{HB})^{-1}\mathbf{H}\boldsymbol{\varepsilon}\mathrm{sgn}(S) \\ &= [(\mathbf{A} - \mathbf{LC})\mathbf{E} + \mathbf{B}\hat{d}_{eq} - \mathbf{v}]^{\mathrm{T}}\mathbf{PE} + \mathbf{E}^{\mathrm{T}}\mathbf{P}[(\mathbf{A} - \mathbf{LC})\mathbf{E} \\ &\quad + \mathbf{B}\hat{d}_{eq} - \mathbf{v}] + (\mathbf{HB})^{-1}\mathbf{H}\boldsymbol{\varepsilon}\,|S|\end{aligned} \tag{9}$$

When $S = \dot{S} = 0$, we have $\mathbf{H}(\mathbf{LC} - \mathbf{BK})\mathbf{E} = \mathbf{H}(\mathbf{B}\hat{d}_{eq} - \mathbf{v})$. According to the properties of inverse matrix of Moore-Penrose, $\mathbf{H}^{+} = (\mathbf{H}^{\mathrm{H}}\mathbf{H})^{+}\mathbf{H}^{\mathrm{H}}$. Therefore,

$$\mathbf{B}\hat{d}_{eq} - \mathbf{v} = (\mathbf{LC} - \mathbf{BK})\mathbf{E} \tag{10}$$

Substituting (10) into (9) yields

$$\begin{aligned}\dot{V}_o &= \dot{\mathbf{E}}^{\mathrm{T}}\mathbf{PE} + \mathbf{E}^{\mathrm{T}}\mathbf{P}\dot{\mathbf{E}} + S\dot{S} \\ &= [(\mathbf{A} - \mathbf{LC})\mathbf{E} + (\mathbf{LC} - \mathbf{BK})\mathbf{E}]^{\mathrm{T}}\mathbf{PE} + \mathbf{E}^{\mathrm{T}}\mathbf{P}[(\mathbf{A} - \mathbf{LC})\mathbf{E} \\ &\quad + (\mathbf{LC} - \mathbf{BK})\mathbf{E}] + (\mathbf{HB})^{-1}\mathbf{H}\boldsymbol{\varepsilon}\,|S| \\ &= \mathbf{E}^{\mathrm{T}}[(\mathbf{A} - \mathbf{BK})^{\mathrm{T}}\mathbf{P} + \mathbf{P}(\mathbf{A} - \mathbf{BK})]\mathbf{E} + (\mathbf{HB})^{-1}\mathbf{H}\boldsymbol{\varepsilon}\,|S| \\ &= -\mathbf{E}^{\mathrm{T}}\mathbf{QE} + (\mathbf{HB})^{-1}\mathbf{H}\boldsymbol{\varepsilon}\,|S|\end{aligned} \tag{11}$$

If $\boldsymbol{\varepsilon}$ is chosen an appropriate value and $(\mathbf{HB})^{-1}\mathbf{H}\boldsymbol{\varepsilon} < 0$, then $\dot{V} < 0$ is met. Therefore, the estimation error of system states asymptotically converges to zero, and the observer is asymptotically stable.

Theorem 1 is proved.

B. DESIGN OF FILTER

In practical engineering, the system output is measured by sensor, and it is inevitable to introduce the measurement noise [29], [30]. In order to facilitate the realization of project and reduce the impact of noise in the disturbance estimation, the filter $Q(s)$ is introduced in the output of the EID estimation.

Then, the EID is estimated through LPF as (12)

$$\hat{D}_{eq\_real}(s) = Q(s)\hat{D}_{eq}(s). \tag{12}$$

where $\hat{D}_{eq\_real}(s)$ and $\hat{D}_{eq}(s)$ are the Laplace transforms of $\hat{d}_{eq\_real}(t)$ and $\hat{d}_{eq}(t)$, respectively. Combining the disturbance estimate (12) with the control law (4) becomes

$$u(t) = u_r(t) - \hat{d}_{eq\_real}(t) \tag{13}$$

Combining (2), (3), and (13) with the aforementioned equation yields

$$\dot{\mathbf{E}} = (\mathbf{A} - \mathbf{LC})\mathbf{E} + \mathbf{B}\hat{d}_{eq\_real}(t) - \mathbf{v} \tag{14}$$

According to (8), we have

$$\hat{d}_{eq}(t) = (\mathbf{HB})^{-1}\mathbf{H}(\mathbf{LC} - \mathbf{BK})\mathbf{E} + (\mathbf{HB})^{-1}\mathbf{H}\boldsymbol{\varepsilon}\mathrm{sgn}(S) \tag{15}$$

By (14) and (15), we have

$$\begin{aligned}&\hat{D}_{eq}(s) \\ &= (\mathbf{HB})^{-1}\mathbf{H}(\mathbf{LC} - \mathbf{BK})[s\mathbf{I} - (\mathbf{A} - \mathbf{LC})]^{-1}\mathbf{B}\hat{D}_{eq\_real}(s) \\ &\quad - \Big\{(\mathbf{HB})^{-1}\mathbf{H}(\mathbf{LC} - \mathbf{BK})[s\mathbf{I} - (\mathbf{A} - \mathbf{LC})]^{-1}\boldsymbol{\varepsilon} \\ &\quad + (\mathbf{HB})^{-1}H\boldsymbol{\varepsilon}\Big\}\,\mathrm{sgn}(S)\end{aligned} \tag{16}$$

Define $G_{dis}(s)$ as the transfer function from $\hat{d}_{eq\_est}(t)$ to $\hat{d}_{eq}(t)$, and $G_{sgn}(s)$ as the transfer function from $sgn(S)$ to $\hat{d}_{eq}(t)$. Then

$$\begin{cases} G_{dis}(s) = (\mathbf{HB})^{-1}\mathbf{H}(\mathbf{LC} - \mathbf{BK})[s\mathbf{I} - (\mathbf{A} - \mathbf{LC})]^{-1}\mathbf{B} \\ G_{sgn}(s) = -(\mathbf{HB})^{-1}\mathbf{H}(s\mathbf{I} + 2\mathbf{LC} - \mathbf{BK} - \mathbf{A}) \\ \qquad [s\mathbf{I} - (\mathbf{A} - \mathbf{LC})]^{-1}\boldsymbol{\varepsilon} \end{cases} \tag{17}$$

According to the small gain theorem[31], a system with NSMDOB is stable if $\|G_{dis}(j\omega)Q(j\omega)\|_{\infty} \leq 1$.

Accordingly, the LFP $Q(s)$ has a direct impact on the stability of SMDOB. The LFP $Q(s)$ is designed as (18).

$$Q(s) = \frac{g_c}{s + g_c} \tag{18}$$

where g_c is the cut off frequency of the first order filter.

III. SYSTEM MODEL DESCRIPTION OF PHOTOELECTRIC TRACKING PLATFORM BASED ON ADDITIVE DECOMPOSITION

Consider the photoelectric tracking platform driven by DC torque motor. The dynamic equation of the plant can be described as

$$J\ddot{x} = -B\dot{x} + u + d_{ext} \tag{19}$$

where J, B, x and u denote the inertia mass, damping, angular position response, and control input, respectively. d_{ext} denotes the disturbance such as nonlinear friction, torque from the environment and dynamic uncertainty. This is the reason why it is difficult to bulid a mathematical model of the disturbance. Here, parameter variability and external disturbances are considered in (19), then (19) is transformed into

$$\begin{cases} \dot{\mathbf{x}}(\mathbf{t}) = [\mathbf{A} + \Delta\mathbf{A}]\mathbf{x}(\mathbf{t}) + [\mathbf{B} + \Delta\mathbf{B}](u(t) + d_{ext}(t)) \\ y = [\mathbf{C} + \Delta\mathbf{C}]\mathbf{x}(\mathbf{t}) \\ e(t) = -[\mathbf{C} + \Delta\mathbf{C}]\mathbf{x}(\mathbf{t}) + r(t) \end{cases} \tag{20}$$

where, $\mathbf{x} = \begin{bmatrix} x_1 & x_2 \end{bmatrix}^{\mathbf{T}} = \begin{bmatrix} x & \dot{x} \end{bmatrix}^{\mathbf{T}}$, $\mathbf{A} = \begin{bmatrix} 0 & 1 \\ 0 & -\frac{B_n}{J_n} \end{bmatrix}$, $\mathbf{B} = \begin{bmatrix} 0 & \frac{1}{J_n} \end{bmatrix}^{\mathrm{T}}$, $\mathbf{C} = \begin{bmatrix} 1 & 0 \end{bmatrix}$. J_n and B_n respectively denote the nominal mass and nominal damping. $\Delta\mathbf{A}$, $\Delta\mathbf{B}$ and $\Delta\mathbf{C}$ express the time-varying bounded uncertainty matrix. $r(t)$ is the system tracking command, and $e(t) = r(t) - x(t)$is the tracking error. (20) can be rewritten as

$$\begin{cases} \dot{\mathbf{x}(\mathbf{t})} = [\mathbf{A} + \Delta\mathbf{A}]\mathbf{x}(\mathbf{t}) + \mathbf{B}(u(t) + d_{eq}(t)) \\ y = \mathbf{C}\mathbf{x}(\mathbf{t}) \\ e(t) = -[\mathbf{C} + \Delta\mathbf{C}]\mathbf{x}(\mathbf{t}) + r(t) \end{cases} \tag{21}$$

where, $d_{eq}(t)$ is the EID given by

$$\mathbf{B}d_{eq}(t) = [\mathbf{B} + \Delta\mathbf{B}]d_{ext}(t) + \Delta\mathbf{B}u(t).$$

A NSMDOB for (21) is designed as (22).

$$\begin{cases} \hat{d}_{eq}(t) = (\mathbf{HB})^{-\mathbf{1}}\mathbf{H}(\mathbf{LC} - \mathbf{BK})\mathbf{E} + (\mathbf{HB})^{-\mathbf{1}}\mathbf{H}\mathbf{v} \\ \hat{D}_{eq\_real}(s) = Q(s)\hat{D}_{eq}(s) \end{cases} \tag{22}$$

where $\mathbf{E} = \hat{\mathbf{x}} - \mathbf{x}$, $\hat{\mathbf{x}}$ is the state observation of $\mathbf{x}$.

Substituting $\hat{d}_{eq}(t)$ into (21), then plant is expressed as (23).

$$\begin{cases} \dot{\mathbf{x}}(t) = [\mathbf{A} + \Delta\mathbf{A}]\,\mathbf{x}(t) + \mathbf{B}[u_r + u_s + \tilde{d}_{eq}(t)] \\ y(t) = \mathbf{C}\mathbf{x}(t) \end{cases} \tag{23}$$

Define the disturbance estimation error as

$$\tilde{d}_{eq}(t) = d_{eq}(t) - \hat{d}_{eq}(t).$$

If $\hat{d}_{eq} = d_{eq}$, then $\tilde{d}_{eq} = 0$ is met. Because the NSMDOB has the problem of the uncompensated disturbance in fact, the estimation error of the EID is not zero. Then, the system dynamic equation is given by

$$J_n\ddot{x} + B_n\dot{x} = u_r + u_s + \delta(t) \tag{24}$$

where $\delta(t)$ is an uncertainty item, and

$$\mathbf{B}\delta(t) = \Delta\mathbf{A}\mathbf{x}(t) + \mathbf{B}\tilde{d}_{eq}(t).$$

According to the additive decomposition theory [20], the system (21) is decomposed. Define a main system as

$$\begin{cases} \dot{\mathbf{x}}_p(t) = \mathbf{A}\mathbf{x}_p(t) + \mathbf{B}u_p(t) \\ y_p(t) = \mathbf{C}\mathbf{x}_p(t) \\ e_p(t) = -\mathbf{C}\mathbf{x}_p(t) + r(t), \quad \mathbf{x}_p(0) = 0 \end{cases} \tag{25}$$

where $\mathbf{x}_p(t) = \begin{bmatrix} x_{p,1} & x_{p,2} \end{bmatrix}^{\mathrm{T}}$ is the state variable of the main system, and $u_p = u_r$ is the control law of the main system. Then, the main system can be expressed as

$$J_n\ddot{x}_{p,1} + B_n\dot{x}_{p,1} = u_r \tag{26}$$

By subtracting (25) from (23), the auxiliary system is described as (27).

$$\begin{cases} \dot{\mathbf{x}}_s(t) = [\mathbf{A} + \Delta\mathbf{A}]\,\mathbf{x}_s(t) + \Delta\mathbf{A}\mathbf{x}_p(t) + \mathbf{B}\left[u_s + \tilde{d}_{eq}(t)\right] \\ = \mathbf{A}\mathbf{x}_s(t) + \mathbf{B}u_s + \mathbf{B}\delta(t) \\ y_s(t) = \mathbf{C}\mathbf{x}_s(t) \\ e_s(t) = -\mathbf{C}\mathbf{x}_s(t), \quad \mathbf{x}_s(0) = \mathbf{x}_o \end{cases} \tag{27}$$

where $\mathbf{x}_s(t) = \begin{bmatrix} x_{s,1} & x_{s,2} \end{bmatrix}^{\mathrm{T}}$ and u_s are the state variable and control law of the auxiliary system, respectively. The auxiliary system dynamic equation is given by

$$J_n\ddot{x}_{s,1} + B_n\dot{x}_{s,1} = u_s + \delta(t) \tag{28}$$

On the basis of additive decomposition theory, we have $\mathbf{x} = \mathbf{x}_p + \mathbf{x}_s$ and $y = y_p + y_s$. From the decomposition structure, we know that the uncertainty item of the system is decomposed into the auxiliary system. The controller of the main system is designed to realize the instruction tracking. The compensator of the auxiliary system is designed to ensure the robustness and stability. Therefore, $y = y_p + y_s \rightarrow r(t)$ is met. The control tasks of the photoelectric tracking system are decomposed and the design objectives are cleared by the additive decomposition.

The whole control structure of the photoelectric tracking platform is shown in Fig.2. The NSMDOB-based compound control with the additive decomposition is applied to the photoelectric tracking platform system. The design methods of $u_p(t)$ and $u_s(t)$ are introduced in section IV.

IV. DESIGN OF CONTROLLER OF MAIN SYSTEM AND COMPENSATOR OF AUXILIARY SYSTEM

A. DESIGN OF CONTROLLER OF MAIN SYSTEM

So far, control tasks discussed are expressed as function of: ①position. ②velocity. ③position +velocity. ④position

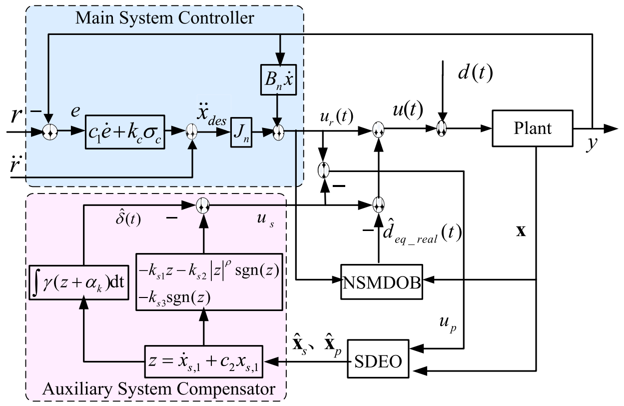

FIGURE 2. **The control structure of the closed-loop system.**

+velocity +acceleration. The design had been presented at two different levels —one based on intuitive reasoning and another based on the enforcement of the desired Lyapunov stability conditions with asymptotic or finite-time convergence. Both solutions are shown to lead to acceleration control structure. In order to select the appropriate control torque to enforce stability of the equilibrium solution for a generalized control error, this paper selects acceleration force with a generalized output control error as the control input. The control structure of the closed-loop system is shown in Fig. 2.

Define a tracking error of system variable e as $e = y - r = x - r$. Suppose r has a two-order time derivative. Define the generalized error σ_c as

$$\sigma_c = \dot{e} + c_1 e \tag{29}$$

where c_1 is a positive constant. If we want to make σ_c asymptotically converges to zero, then the closed-loop system dynamics are determined by the convergence law $\dot{\sigma}_c + k_c\sigma_c = 0$, where k_c is the proportional gain coefficient. Therefore, the design of control law in the system (26) can be divided into two-step processes: the design of equivalent acceleration $\ddot{x}_{eq}$ and the design of convergence acceleration $\ddot{x}_{con}$. The desired acceleration of the system is given by $\ddot{x}_{des} = \ddot{x}_{eq} + \ddot{x}_{con}$. $\ddot{x}_{eq}$ is a specific task, thus it can be derived from a known control output. $\ddot{x}_{con}$ is specified by the desired convergence law.

To ensure $\dot{\sigma}_c = 0$, then $\ddot{x}_{eq} = \ddot{x}_{ref} - c\dot{e}$. Let $\ddot{x}_{con} = -k_c\sigma_c$, then dynamic closed-loop system $\dot{\sigma}_c + k_c\sigma_c = 0$. The desired acceleration is expressed as

$$\ddot{x}_{des} = \ddot{x}_{ref} - c\dot{e} - k_c\sigma_c \tag{30}$$

According to (30), the control law of the main system can be designed as

$$u_r = J_n[\frac{B_n}{J_n}\dot{x} + \ddot{x}_{des}] = J_n[\ddot{x}_{ref} - k_c\sigma_c - (c\dot{e})] + B_n\dot{x} \tag{31}$$

B. DESIGN OF CONTROLLER OF AUXILIARY SYSTEM

From the results of the model decomposition, it can be seen that uncertain and uncompensated disturbances exist in the auxiliary system. The compensator needs to be designed to compensate the uncertain and uncompensated disturbances, so as to achieve the stability of the auxiliary system.

The design goal of u_s is to make $\mathbf{x_s} \to 0$, that is $u_s \to \delta(t)$. Define the sliding mode surface of the auxiliary system

$$z = \dot{x}_{s,1} + c_2 x_{s,1} \tag{32}$$

where $c_2 = \frac{B_n}{J_n}$. Here, the design goal is $z \to 0$. Define control law as

$$\begin{cases} u_s = -k_{s1}z - k_{s2}\,|z|^\rho\,\mathrm{sgn}(z) - k_{s3}\mathrm{sgn}(z) - \hat{\delta}(t) \\ \dot{\hat{\delta}}(t) = \gamma(z + \alpha_k) \end{cases} \tag{33}$$

where $k_{s1} > 0$, $k_{s2} > 0$, $k_{s3} > 0$, $0 < \rho < 1$, $\gamma > 0$ and $\alpha_k > 0$. k_{s1} determines the convergence speed of the sliding mode control. k_{s2} and k_{s3} ensure the reachability of the finite time. $\hat{\delta}(t)$ is the estimated value of $\delta(t)$, which is used to compensate the uncertainties in the system. Define the estimated error as $\tilde{\delta}(t) = \delta(t) - \hat{\delta}(t)$, then $\dot{\tilde{\delta}}(t) = -\dot{\hat{\delta}}(t)$.

Lemma 1 [32]: Consider $\dot{x} = f(t, x), t \geq 0, x \in \Re^n$, where $f(\cdot) : \Re^{1+n} \to \Re^n$ is continuous and $f(t, 0) = 0$. Suppose that there exists a positive definite and proper function $V(t) : \Re^n \to \Re$ such that $\dot{V}(t) \leq -\alpha V^\eta(t)$ where $\alpha > 0, 0 < \eta < 1$. For arbitrary given t_o, there is a finite time. Then the origin of the system is globality and uniformity finite time table. The settling time satisfies $t_1 \leq t_o + \frac{V^{1-\eta}(t_o)}{\alpha(1-\eta)}$.

Theorem 2: For system (23) with uncertain disturbance, emply the additive decomposition theory. The system is divided into the main system (26) and the auxiliary system (28). If the control law is (31) in the main system and the control law is designed as (33) in the auxiliary system, then the following conclusions are made.

(1) The sliding surface (32) converges to zero in finite time.
(2) $\mathbf{x_s}$ convergences to a small range in finite time and exponentially convergences to zero, that is $\lim_{t\to\infty} \|\mathbf{x}_s\| = 0$.
(3) The closed-loop system (24) is asymptotic stabilization.
(4) $\lim_{t\to\infty} y = r$, $\lim_{t\to\infty} y_p = r$ and $\lim_{t\to\infty} \dot{y}_p = 0$.

Proof: Define a positive definite Lyapunov candidate (34).

$$V_s = \frac{1}{2}J_n z^2 + \frac{1}{2\gamma}\tilde{\delta}(t)^2 \tag{34}$$

Then, the time derivation of V_s is deduced as (35)

$$\begin{aligned} \dot{V}_s &= zJ_n\dot{z} + \frac{1}{\gamma}\tilde{\delta}(t)\dot{\tilde{\delta}}(t) \\ &= zJ_n(\ddot{x}_{s,1} + c_2\dot{x}_{s,1}) - \frac{1}{\gamma}[\delta(t) - \hat{\delta}(t)]\dot{\hat{\delta}}(t) \\ &= z[u_s + \delta(t)] - \frac{1}{\gamma}[\delta(t) - \hat{\delta}(t)]\dot{\hat{\delta}}(t) \\ &= -k_{s1}z^2 - k_{s2}\,|z|^\rho\,z\mathrm{sgn}(z) - k_{s3}z\mathrm{sgn}(z) + z[\delta(t) - \hat{\delta}(t)] \\ &\quad - \frac{1}{\gamma}[\delta(t) - \hat{\delta}(t)]\dot{\hat{\delta}}(t) \end{aligned}$$

$$
\begin{aligned}
&= -k_{s1}z^2 - k_{s2}|z|^{\rho+1} - k_{s3}|z| + [\delta(t) - \hat{\delta}(t)][z - \frac{1}{\gamma}\dot{\hat{\delta}}(t)] \\
&\leq -k_{s1}z^2 - k_{s2}|z|^{\rho+1} - k_{s3}|z| + \left|\delta(t) - \hat{\delta}(t)\right| [z - \frac{1}{\gamma}\dot{\hat{\delta}}(t)]
\end{aligned}
\tag{35}
$$

Introduce a parameter $\alpha_k > 0$, then

$$
\begin{aligned}
\dot{V}_s &\leq -k_{s1}z^2 - k_{s2}|z|^{\rho+1} - k_{s3}|z| - \alpha_k\left|\delta(t) - \hat{\delta}(t)\right| \\
&\quad + \alpha_k\left|\delta(t) - \hat{\delta}(t)\right| + \left|\delta(t) - \hat{\delta}(t)\right| [z - \frac{1}{\gamma}\dot{\hat{\delta}}(t)] \\
&= -k_{s1}z^2 - k_{s2}|z|^{\rho+1} - k_{s3}|z| - \alpha_k\left|\delta(t) - \hat{\delta}(t)\right| \\
&\quad - \left|\delta(t) - \hat{\delta}(t)\right| [\frac{1}{\gamma}\dot{\hat{\delta}}(t) - z - \alpha_k] \\
&\leq -k_{s3}|z| - \alpha_k\left|\delta(t) - \hat{\delta}(t)\right| - \left|\delta(t) - \hat{\delta}(t)\right| \\
&\quad \times [\frac{1}{\gamma}\dot{\hat{\delta}}(t) - z - \alpha_k]
\end{aligned}
\tag{36}
$$

According to (33), (36) becomes

$$
\begin{aligned}
\dot{V}_s &\leq -k_{s3}|z| - \alpha_k\left|\delta(t) - \hat{\delta}(t)\right| \\
&= -\frac{\sqrt{2}/2}{-}\alpha_k\sqrt{2\gamma}\frac{\left|\delta(t) - \hat{\delta}(t)\right|}{\sqrt{2\gamma}} \\
&\leq -\alpha V_s^{\frac{1}{2}}
\end{aligned}
\tag{37}
$$

where $\alpha = \min\left\{\frac{\sqrt{2}k_{s3}}{\sqrt{J_n}},\ \alpha_k\sqrt{2\gamma}\right\}$.

Therefore, $\dot{V}_s \leq -\alpha V_s^{\frac{1}{2}} \leq 0$ is met. According to lemma 1, there is a finite time t_1 in which the sliding mode surface (32) converges to zero. The convergence time is $t_1 = t_o + \frac{2V^{\frac{1}{2}}(t_o)}{\alpha}$. Due to $z = \dot{x}_{s,1} + c_2x_{s,1}$, $x_{s,1}(t)$ quickly converges to a small range in a finite time. Then, $x_{s,1}(t)$ is the exponential convergence to zero, that is $\lim_{t\to\infty}\|x_s\| = 0$.

In order to discuss the stability of closed-loop system, a Lyapunov function of the closed loop system is chosen: $V_c = \frac{1}{2}\sigma_c$, then $\dot{V}_c = \sigma_c\dot{\sigma}_c = -k_c\sigma_c^2 < 0$. Obviously, the closed-loop system (24) is asymptotic stabilization.

According to the solving process, we have

$$
|\sigma_c(t)| = |\sigma_c(0)|\exp(-2k_ct) \tag{38}
$$

It is means that σ_c converges to zero exponentially. According to the definition of $\sigma_c = \dot{e} + c_1e$, e asymptotically decays to zero. Then, $\lim_{t\to\infty} y = r = x$. Due to $\mathbf{x} = \mathbf{x}_p + \mathbf{x}_s$, we have $\lim_{t\to\infty}\mathbf{x}_p = \lim_{t\to\infty}(\mathbf{x} - \mathbf{x}_s) = \mathbf{x}$. Therefore, $\lim_{t\to\infty} y_p = r$ and $\lim_{t\to\infty}\dot{y}_p = 0$ is met.

Theorem 2 is proved.

In this method, the sliding mode compensator helps the NSMDOB to estimate the disturbance. Here, the compensator includes the adaptive law of the uncertainties $\delta(t)$. The switching gain k_{s3} is only required to be a small value. Thus chattering can be alleviated. In engineering practice, the sgn(z) is replaced by the saturation function (41) to weaken the chattering further.

$$
\operatorname{sat}\left(\frac{x}{\Delta}\right) = \begin{cases} 1, & x > \Delta \\ \frac{x}{\Delta}, & |x| \leq \Delta \\ -1, & x < -\Delta \end{cases} \tag{39}
$$

where Δ is the width of a boundary layer. Employing the saturation function, the control law changes from (33) to (40).

$$
\begin{cases} u_s = -k_{s1}z - k_{s2}|z|^{\rho}\operatorname{sat}(\frac{z}{\varepsilon}) - k_{s3}\operatorname{sat}(\frac{z}{\varepsilon}) - \hat{\delta}(t) \\ \dot{\hat{\delta}}(t) = \gamma(z + \alpha_k) \end{cases} \tag{40}
$$

where ε is a small positive constant. The parameter k_{s1}, k_{s3} and k_{s2} are selected according to a certain rule, that is k_{s1} and k_{s3} is greater than k_{s2}.

Theorem 3: For system (23) with uncertain disturbance, employ additive decomposition theory. The system is divided into the main system (26) and the auxiliary system (28). If the control law is (31) in the main system and the control law is designed as (40) in the auxiliary system, then the auxiliary system is asymptotically stable.

Proof: Define a positive definite Lyapunov candidate

$$
V_s = \frac{1}{2}J_nz^2 + \frac{1}{2\gamma}\tilde{\delta}(t)^2 \tag{41}
$$

Then, the time derivation of V_s is deduced as (42).

$$
\begin{aligned}
\dot{V}_s &= zJ_n\dot{z} + \frac{1}{\gamma}\tilde{\delta}(t)\dot{\hat{\delta}}(t) \\
&= -k_{s1}z^2 - k_{s2}|z|^{\rho} z\operatorname{sat}(\frac{z}{\varepsilon}) - k_{s3}z\operatorname{sat}(\frac{z}{\varepsilon}) \\
&\quad + z[\delta(t) - \hat{\delta}(t)] - \frac{1}{\gamma}[\delta(t) - \hat{\delta}(t)]\dot{\hat{\delta}}(t) \\
&\leq -k_{s1}z^2 - k_{s2}|z|^{\rho} z\operatorname{sat}(\frac{z}{\varepsilon}) - k_{s3}z\operatorname{sat}(\frac{z}{\varepsilon}) \\
&\quad + \left|\delta(t) - \hat{\delta}(t)\right| [z - \frac{1}{\gamma}\dot{\hat{\delta}}(t)]
\end{aligned}
\tag{42}
$$

If $|z| \geq \varepsilon$, then $\operatorname{sat}\left(\frac{z}{\varepsilon}\right) = \operatorname{sgn}(z)$. According to the proof of theorem 2, $\dot{V}_s \leq -k_{s1}z^2 \leq 0$ is met. Therefore, z is asymptotic convergence until $|z| < \varepsilon$.

When $|z| < \varepsilon$, $\operatorname{sat}\left(\frac{z}{\varepsilon}\right) = \frac{z}{\varepsilon}$. We have

$$
\dot{V}_s \leq -k_{s1}z^2 - \frac{k_{s2}}{\varepsilon}|z|^{\rho+2} - \frac{k_{s3}}{\varepsilon}z^2 + \left|\delta(t) - \hat{\delta}(t)\right| [z - \frac{1}{\gamma}\dot{\hat{\delta}}(t)]
$$

Introduce a parameter $\alpha_k > 0$, then

$$
\begin{aligned}
\dot{V}_s &\leq -k_{s1}z^2 - \frac{k_{s2}}{\varepsilon}|z|^{\rho+2} - \frac{k_{s3}}{\varepsilon}z^2 - \alpha_k\left|\delta(t) - \hat{\delta}(t)\right| \\
&\quad + \alpha_k\left|\delta(t) - \hat{\delta}(t)\right| + \left|\delta(t) - \hat{\delta}(t)\right| [z - \frac{1}{\gamma}\dot{\hat{\delta}}(t)] \\
&= -k_{s1}z^2 - \frac{k_{s2}}{\varepsilon}|z|^{\rho+2} - \frac{k_{s3}}{\varepsilon}z^2 - \alpha_k\left|\delta(t) - \hat{\delta}(t)\right| \\
&\quad - \left|\delta(t) - \hat{\delta}(t)\right| [\frac{1}{\gamma}\dot{\hat{\delta}}(t) - z - \alpha_k] \\
&\leq -k_{s1}z^2 - \frac{k_{s2}}{\varepsilon}|z|^{\rho+2} - \frac{k_{s3}}{\varepsilon}z^2 - \alpha_k\left|\delta(t) - \hat{\delta}(t)\right| \\
&\quad - \left|\delta(t) - \hat{\delta}(t)\right| [\frac{1}{\gamma}\dot{\hat{\delta}}(t) - z - \alpha_k] \\
&\leq 0
\end{aligned}
\tag{43}
$$

FIGURE 3. The three-axis LOS motion control device.

Therefore, the auxiliary system is asymptotically stable. And $x_{s,1}(t)$ is the asymptotic convergence to zero.

Theorem 3 is proved.

C. STATE DECOMPOSITION OBSERVER (SDEO)

When a controller is designed based on the model decomposition, it is needed to consider that $\mathbf{x}_s(t)$ cannot be measured directly. By taking this into account, the state decomposition observer (SDEO) is proposed to observe the state $\mathbf{x}_p(t)$ and $\mathbf{x}_s(t)$.

Let the SDEO is designed as follows

$$\begin{cases} \dot{\hat{\mathbf{x}}}_p(t) = \mathbf{A}\hat{\mathbf{x}}_p(t) + \mathbf{B}u_p(t) \\ \hat{\mathbf{x}}_s(t) = \mathbf{x}(t) - \hat{\mathbf{x}}_p(t), \qquad \hat{\mathbf{x}}_p(0) = 0 \end{cases} \tag{44}$$

Subtracting (44) from (25), the results is as follows

$$\dot{\tilde{\mathbf{x}}}_p(t) = \mathbf{A}\tilde{\mathbf{x}}_p(t), \quad \tilde{\mathbf{x}}_p(0) = 0 \tag{45}$$

where $\tilde{\mathbf{x}}_p = \hat{\mathbf{x}}_p - \mathbf{x}_p$. If $\mathbf{A}$ meets stability condition, then $\hat{\mathbf{x}}_p \equiv \mathbf{x}_p$ and $\mathbf{x}_s = \mathbf{x} - \mathbf{x}_p = \mathbf{x} - \hat{\mathbf{x}}_p = \hat{\mathbf{x}}_s$.

In the above design, the EID is estimated and compensated in (21) at first, and then (23) is decomposed. At this point, the control task of the system is decomposed into the tracking subtask for the main system and the stabilization subtask for the auxiliary system. It is worth mentioning that the compensator compensates the uncompensated EID in the auxiliary system.

V. SIMULATIONS AND EXPERIMENTS

In order to test the effect of the proposed method, the simulations and experiments were implemented. The effectiveness of NSMDOB for the EID estimation is verified in this section. The experimental setup and experimental results are illustrated in this sections A and C, respectively.

A. EXPERIMENTAL SETUP

The experiments were implemented by using a three-axis LOS motion control device shown in Fig. 3. The position information was measured by the optical-electrical encoder with resolution of 0.0007 degrees. The program of control algorithm was written in C language based on Windows-RTX real-time system in an industrial computer. The sampling time was 0.001s.

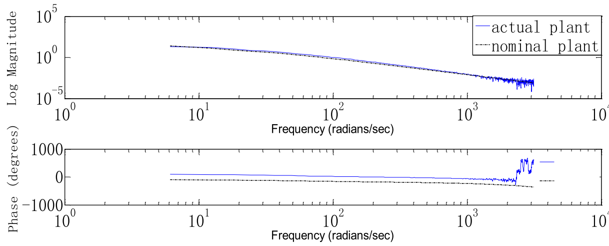

FIGURE 4. The fitting curves for frequency characteristics of actual plant and nominal model.

TABLE 1. Experimental parameters.

Parameters	Value
Observer gain matrix	$\mathbf{L} = [15\ \ 50]^T$
Sliding mode surface feedback matrix	$\mathbf{K} = [10\ \ 0.01]$
Positive constant matrix	$\mathbf{H} = [1\ \ 0.5]$
Switching law gain matrix	$\boldsymbol{\varepsilon} = [-0.1\ \ 0.02]^T$
Proportional gain coefficient	$k_c = 130$
Constant gain	$c_1 = -220$
Constant gain	$\rho = 0.5$
Constant	$\alpha_k = 0.001$
Sliding mode control constant gain 1	$k_{s1} = 0.01$
Sliding mode control constant gain 2	$k_{s2} = 0.005$
Sliding mode control constant gain 2	$k_{s3} = 0.02$
Boundary layer width	$\varepsilon = 0.001$
Adaptive law coefficient	$\gamma = 0.5$
Q(S) cutoff frequency	$g_c = 100$

The pitch axis was chosen herein to verify the method proposed in the paper because each axis of the photoelectric tracking platform could be designed independently. The parameters of the nominal model were identified as $J_n = 0.00014\ kg$ and $B_n = 0.0071\ N \cdot s \cdot m^{-1}$ by the white noise frequency sweep method. The fitting curves for frequency characteristics of actual plant and nominal model are shown in Fig. 4. Other parameters are shown in Table 1.

The friction interference is the main disturbance of the electromechanical servo system at the low speed of the system. In order to analyze friction characteristics of the plant, we tested the dead zone characteristics of the internal friction for the photoelectric tracking platform. In the open-loop control system, we added directly the different output voltage to the D/A output, which was started from 0.15V and increased 0.01V output voltage every 2 seconds. Fig. 5 illustrates that the motor starts to move when the system voltage is increased to 0.2V. It shows that the control system has a certain range of the control dead zone due to the influence of the friction and other disturbances in the electromechanical servo system. Therefore, we observed that the disturbance $d_{ext}(x, \dot{x}, t)$ is a strong nonlinearity function of the relation x, $\dot{x}$ and t.

B. NUMERICAL SIMULATION RESULT

In this section, the simulation results of the proposed NSMDOB scheme are compared with the conventional DOB scheme[7], with respect to the accuracy of the EID estimation.

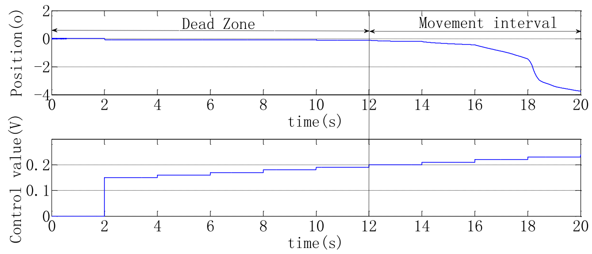

FIGURE 5. Friction dead zone characteristic test curve.

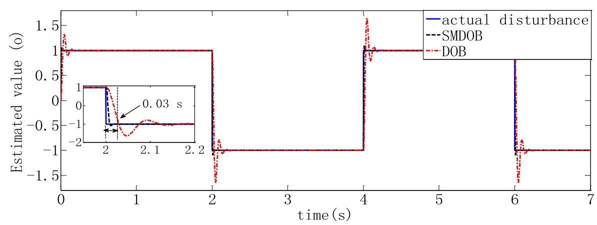

(a) Square wave signal disturbance

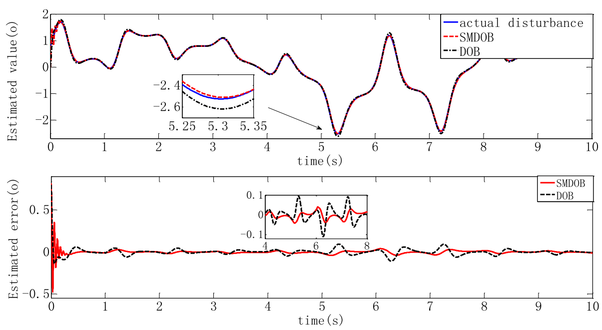

(b) Arbitrary signal disturbance

FIGURE 6. Comparison curves of the disturbance estimation.

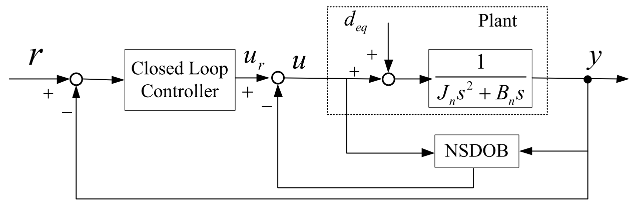

FIGURE 7. NSMDOB-based compound control structure.

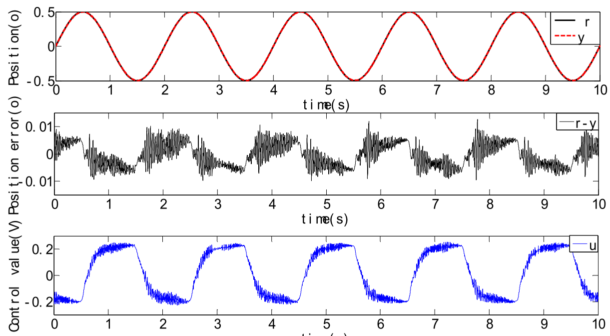

(a) NSMDOB-based compound control

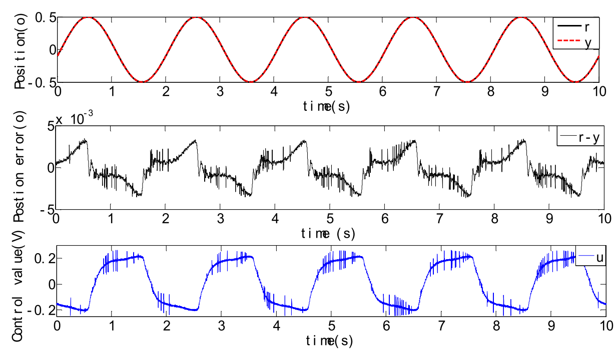

(b) NSMDOB-based compound control with additive decomposition

FIGURE 8. Comparison curves under two scheme with sinusoidal input (A=0.50, f=0.5Hz).

The simulations were carried out in the MATLAB software environment. The parameters of Table 1 were employed in the following simulations.

Fig. 6 illustrates the results when the DOB and NSMDOB are employed. The NSMDOB can quickly estimate the mutation disturbance, and the estimated accuracy of NSMDOB is better than DOB. The NSMDOB method may effectively estimate the low frequency and high frequency component of the disturbance. At the same time, the speed of disturbance estimation may be adjusted by selecting the parameters of NSMDOB. Since it has a switching control, the sliding mode technique may reject the impact of nonlinear disturbance in high frequency domain, which is not compensated well by the DOB. Therefore, the proposed control scheme enhances the system robustness.

C. EXPERIMENTAL RESULTS

For comparison, the NSMDOB-based compound control and the NSMDOB-based compound control with additive decomposition were both implemented. The control structure of the NSMDOB-based compound control is shown in Fig. 7. The closed loop controller u_r is designed as (31) in Fig. 7.

Fig. 8 compares the tracking error and control value of two control schemes when the reference input signal is a sinusoidal signal. The sinusoidal signal's amplitude was 0.5 degree and it's frequency was 0.5Hz. The results indicate that the NSMDOB-based compound control with additive decomposition may achieve a better position tracking performance than the SMDOB-based compound control. The maximum tracking error decreased from 0.01 degree to 0.0034 degree with the help of the sliding mode compensator. The compensator achieves the adjustment to $\mathbf{x}_s$ better. From Fig. 8, we can see that the tracking error reaches the maximum value at zero velocity, and the tracking error of the proposed control scheme with additive decomposition is smaller. Fig.8 illustrates that the controller output curve of the compound control scheme with additive decomposition is smoother than the SMDOB-based compound control scheme.

In order to test the dynamic performance, the tracking command signal was employed as $0.5\sin(8\pi t)$. Fig. 9 shows

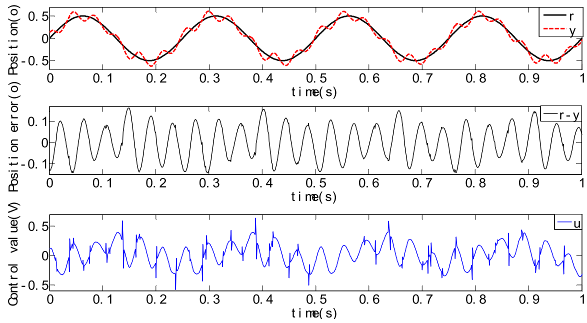

(a) NSMDOB-based compound control

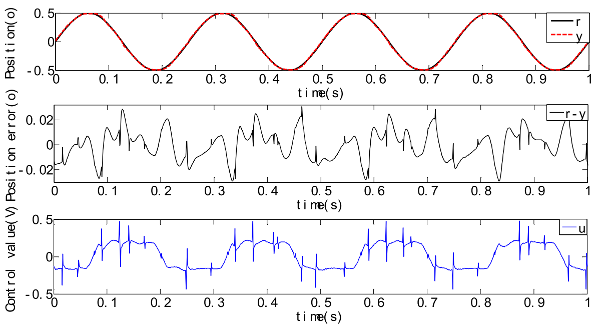

(b) NSMDOB-based compound control with additive decomposition

FIGURE 9. Comparison curves under two scheme with sinusoidal input (A=0.50, f=4Hz).

the maximum tracking error decreases from 0.14 degree to 0.03 degree.

The result of the tracking error indicates that the compound control scheme with additive decomposition has better dynamic performance. The testing standard of photoelectric tracking platform is satisfied that the maximum tracking error do not exceed 10% of the amplitude of the reference signal in working band. Obviously, the tracking errors of Fig. 8 and Fig. 9 meet this standard under the proposed method with additive decomposition. Furthermore, according to Fig.8 and Fig. 9, the control value of the proposed method is far less than the limit of the D/A converter. We ignore the influence on the small chatting in the responses because the switching gains are small enough. When the sliding mode compensator effectively compensated for $\tilde{d}_{eq}$, the tracking error was effectively decreased. The compensator relieves the work burden of the NSMDOB. The sliding gains are greatly related to the upper bound on the disturbance estimation error, and the small switching gain helps to alleviate the chattering. Furthermore, the EID is fully estimated in finite time. The results indicate that the proposed method in this paper may be reliably performed in practical application.

VI. CONCLUSION

To obtain the high performance and good robustness for ordinary photoelectric tracking platform, this paper proposed the design method of the NSMDOB-based compound control with additive decomposition. Compared with the NSMDOB-based compound control scheme, the compound control scheme with additive decomposition has better tracking performance and robustness.

The proposal does not involve changing the hardware of the LOS motion control device. It presents the method of fine disturbance compensation. The NSMDOB sufficiently compensates the disturbance. The compensator simultan-eously ensures that the EID is effectively estimated in finite time. The design tasks of LOS stabilization and moving target tracking control are simplified and separated by the additive decomposition theory.

Experiments were carried out to validate the proposed control method. The algorithm was realized by programming in a real-time computer system. The experimental results show that the proposed scheme not only ensures the strong robustness against system uncertainties and small tracking error, but also suppresses the high-frequency chattering of the control input effectively. This method may be extended to the relatively high requirements of other servo systems.

As future research, the control system using a more complex model structure can be designed and analyzed. Furthermore, the research content is extended to multi-motor control system and the disturbance compensation is studied from the perspective of interval observation [33], [34].

REFERENCES

[1] J. Fang, R. Yin, and X. Lei, "An adaptive decoupling control for three-axis gyro stabilized platform based on neural networks," *Mechatronics*, vol. 27, pp. 38–46, Apr. 2015.

[2] S. Pan, "Robust control of gyro stabilized platform driven by ultrasonic motor," *Sens. Actuators A, Phys.*, vol. 261, no. 1, pp. 280–287, Jul. 2017.

[3] Y. Zhang, T. Yang, C. Li, S. Liu, C. Du, M. Li, and H. Sun, "Fuzzy-PID control for the position loop of aerial inertially stabilized platform," *Aerosp. Sci. Technol.*, vol. 36, pp. 21–26, Jul. 2014.

[4] Y. Huang and W. Messner, "A novel disturbance observer design for magnetic hard drive servo system with a rotary actuator," *IEEE Trans. Magn.*, vol. 34, no. 4, pp. 1892–1894, Jul. 1998.

[5] Z.-J. Yang, Y. Wang, and S. Kanae, "New approach to an adaptive robust motion controller combined with a disturbance observer," *IET Control Theory Appl.*, vol. 5, no. 10, pp. 1203–1213, Jul. 2011.

[6] V.-P. Vu and W.-J. Wang, "State/disturbance observer and controller synthesis for the T–S fuzzy system with an enlarged class of disturbances," *IEEE Trans. Fuzzy Syst.*, vol. 26, no. 6, pp. 3645–3659, Dec. 2018.

[7] W. Kim, D. Shin, D. Won, and C. C. Chung, "Disturbance-observer-based position tracking controller in the presence of biased sinusoidal disturbance for electrohydraulic actuators," *IEEE Trans. Control Syst. Technol.*, vol. 21, no. 6, pp. 2290–2298, Nov. 2013.

[8] J.-H. She, X. Xin, and Y. Ohyama, "Estimation of equivalent input disturbance improves vehicular steering control," *IEEE Trans. Veh. Technol.*, vol. 56, no. 6, pp. 3722–3731, Nov. 2007.

[9] M. Wu, B. Xu, W. Cao, and J. She, "Aperiodic disturbance rejection in repetitive-control systems," *IEEE Trans. Control Syst. Technol.*, vol. 22, no. 3, pp. 1044–1051, May 2014.

[10] J. H. She, X. Xin, and Y. D. Pan, "Equivalent-input-disturbance approach—Analysis and application to disturbance rejection in dual-stage feed drive control system," *IEEE/ASME Trans. Mechatronics*, vol. 16, no. 2, pp. 330–340, Mar. 2011.

[11] Y. S. Lu, "Sliding-mode disturbance observer with switching-gain adaptation and its application to optical disk drives," *IEEE Trans. Ind. Electron.*, vol. 56, no. 9, pp. 3743–3750, Jun. 2009.

[12] U. S. Pusadkar, S. D. Chaudhari, P. D. Shendge, and S. B. Phadke, "Linear disturbance observer based sliding mode control for active suspension systems with non-ideal actuator," *J. Sound Vibrat.*, vol. 442, pp. 428–444, Mar. 2019.

[13] Y. Zhu, J. Qiao, and L. Guo, "Adaptive sliding mode disturbance observer-based composite control with prescribed performance of space manipulators for target capturing," *IEEE Trans. Ind. Electron.*, vol. 66, no. 3, pp. 1973–1983, Mar. 2019.

[14] C. Chen, L. Pan, S. Liu, L. Sun, and K. Lee, "A sustainable power plant control strategy based on fuzzy extended state observer and predictive control," *Sustainability*, vol. 10, no. 12, p. 4824, 2018.

[15] B. Zhao, S. Xu, J. Guo, R. Jiang, and J. Zhou, "Integrated strapdown missile guidance and control based on neural network disturbance observer," *Aerosp. Sci. Technol.*, vol. 84, pp. 170–181, Jan. 2019.

[16] X. Huang, W. Lin, and B. Yang, "Global finite-time stabilization of a class of uncertain nonlinear systems," *Automatica*, vol. 41, no. 5, pp. 881–888, May 2005.

[17] C. Zhang, Y. Yan, A. Narayan, and H. Yu, "Practically oriented finite-time control design and implementation: Application to a series elastic actuator," *IEEE Trans. Ind. Electron.*, vol. 65, no. 5, pp. 4166–4176, May 2018.

[18] J. Lyu, Q. Ma, J. Qin, Y. Kang, and W. Xing Zheng, "Finite-time attitude synchronisation for multiple spacecraft," *IET Control Theory Appl.*, vol. 10, no. 10, pp. 1106–1114, Jun. 2016.

[19] A. Oveisi and T. Nestorović, "Robust observer-based adaptive fuzzy sliding mode controller," *Mech. Syst. Signal Process.*, vols. 76–77, pp. 58–71, Aug. 2016.

[20] D. Liu and G.-H. Yang, "Prescribed performance model-free adaptive integral sliding mode control for discrete-time nonlinear systems," *IEEE Trans. Neural Netw. Learn. Syst.*, vol. 30, no. 7, pp. 2222–2230, Jul. 2019, doi: 10.1109/TNNLS.2018.2881205.

[21] T. Jing, F. Chen, and X. Zhang, "Finite-time lag synchronization of time-varying delayed complex networks via periodically intermittent control and sliding mode control," *Neurocomputing*, vol. 199, no. 7, pp. 178–184, Jul. 2016.

[22] L. Yu, J. Huang, and S. Fei, "Robust switching control of the direct-drive servo control systems based on disturbance observer for switching gain reduction," *IEEE Trans. Circuits Syst. II, Exp. Briefs*, vol. 66, no. 8, pp. 1366–1370, Aug. 2019.

[23] Q. Quan, K. Y. Cai, "Additive decomposition and its applications to internal-model-based tracking," in *Proc. 48th IEEE Conf. Decis. Control Held Jointly, 28th Chin. Control Conf.*, Dec. 2009, pp. 817–822.

[24] Q. Quan, D. Yang, H. Hu, and K. Y. Cai, "A new model transformation method and its application to extending a class of stability criteria of neutral type systems," *Nonlinear Anal., Real World Appl.*, vol. 11, no. 5, pp. 3752–3762, 2010.

[25] Q. Quan and K.-Y. Cai, "A filtered repetitive controller for a class of nonlinear systems," *IEEE Trans. Autom. Control*, vol. 56, no. 2, pp. 399–405, Feb. 2011.

[26] Q. Quan, G.-X. Du, and K.-Y. Cai, "Proportional-integral stabilizing control of a class of MIMO systems subject to nonparametric uncertainties by Additive-State-Decomposition dynamic inversion design," *IEEE/ASME Trans. Mechatronics*, vol. 21, no. 2, pp. 1092–1101, Apr. 2016.

[27] Q. Quan and K.-Y. Cai, "Additive-state-decomposition-based tracking control for TORA benchmark," *J. Sound Vibrat.*, vol. 332, no. 20, pp. 4829–4841, Sep. 2013.

[28] Q. Quan, K.-Y. Cai, and H. Lin, "Additive-state-decomposition-based tracking control framework for a class of nonminimum phase systems with measurable nonlinearities and unknown disturbances," *Int. J. Robust Nonlinear Control*, vol. 25, no. 2, pp. 163–178, Jan. 2015.

[29] L. Yu and S. Fei, "Large-screen interactive technology with 3D sensor based on clustering filtering method and unscented Kalman filter," *IEEE Access*, vol. 8, pp. 8675–8680, 2020.

[30] L. Yu, C. Li, and S. Fei, "Any-wall touch control system with switching filter based on 3-D sensor," *IEEE Sensors J.*, vol. 18, no. 11, pp. 4697–4703, Jun. 2018.

[31] J. C. Doyle, B. Francis, and A. R. Tannenbaum, *Feedback Control Theory*. New York, NY, USA: Macmillan, 1992.

[32] Q. Chen, L. Yu, and Y. Nan, "Finite-time tracking control for motor servo systems with unknown dead-zones," *J. Syst. Sci. Complex.*, vol. 26, no. 6, pp. 940–956, Dec. 2013.

[33] J. Hunag, X. Ma, H. Che, and Z. Han, "Further result on interval observer design for discrete-time switched systems and application to circuit systems," *IEEE Trans. Circuits Syst. II, Exp. Briefs*, early access, Dec. 5, 2019, doi: 10.1109/TCSII.2019.2957945.

[34] J. Huang, X. Ma, X. Zhao, H. Che, and L. Chen, "An interval observer design method for asynchronous switched systems," *IET Control Theory Appl.*, to be published, doi: 10.1049/iet-cta.2019.0750.

YAN REN received the B.S. degree in automation specialty and the M.S. degree in control science and engineering from the Inner Mongolia University of Science and Technology, Baotou, China, in 1999 and 2006, respectively, and the Ph.D. degree in navigation, guidance and control from Beihang University, Beijing, China, in 2016.

From 2012 to 2016, she was an Assistant Professor with the School of Information Engineering, Inner Mongolia University of Science and Technology, where she has been a Professor, since 2017. She is the author of two books, more than 30 articles, and holds one patent. Her research interests include control theory and applications, motion control theory and engineering, intelligent control theory and application, and uncertain disturbance of system compensation theory and application.

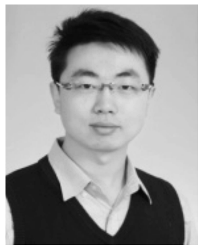

DAPENG TIAN (Senior Member, IEEE) received the B.E. degrees from the Beijing Institute of Technology, Beijing, China, in 2007 and 2012, respectively, and the Ph.D. degree from the Beijing University of Aeronautics and Astronautics (Beihang University), Beijing, in 2012.

He was then directly recommended to study at the Beijing University of Aeronautics and Astronautics (Beihang University). From 2009 to 2012, he was a Co-Researcher with the Advanced Research Center, Keio University, Yokohama, Japan. Since 2012, he has been with the Key Laboratory of Airborne Optical Imaging and Measurement, Changchun Institute of Optics, Fine Mechanics and Physics, Chinese Academy of Sciences, Changchun, China. His current research interests include motion control theory and engineering, optical imaging, and bilateral control. He received the 2017's Outstanding Science and Technology Achievement Prize of the Chinese Academy of Sciences and the 2018's State Science and Technology Award in China.

DAHUA YU was born in Baotou, Inner Mongolia, China, in 1981. He received the Ph.D. degree in pattern recognition and intelligent system from Xidian University, Xi'an, China, in 2013. His research interests include the development of pattern recognition and image processing. His awards and honors include the First Prize, in 2017 and the Second Prize, in 2015 of Natural Science Award of Inner Mongolia, China.